

# Development of an Evaporator Using Porous Wick Structure for a Two-Phase Mechanically Pumped Fluid Loop

Takuro Daimaru<sup>1</sup>, Benjamin Furst<sup>2</sup>, Stefano Cappucci<sup>3</sup>, Eric Sunada<sup>4</sup> and Gajanana Birur<sup>5</sup>  
*NASA Jet Propulsion Laboratory, California Institute of Technology, Pasadena, CA, 91109*

The Jet Propulsion Laboratory is developing a two-phase mechanically pumped fluid loop (2PMPFL) thermal control system to enable novel mission designs and greater science return for NASA. Pumped two-phase fluid loops have the potential to provide robust and effective thermal control that combine the best aspects of passive two-phase systems (heat pipes) and mechanically pumped single-phase fluid loops. The current requirements include the development of a system with multiple 1 m<sup>2</sup> evaporators, each of which is capable of remaining spatially and temporally isothermal while accommodating heat loads of up to 500 W and local fluxes of up to 5 W/cm<sup>2</sup>. The goal is to attain this using less than 5 W of power. Such a system would be able to accommodate the next generation of payload and bus electronics while using minimal resources.

## Nomenclature

$A$	=	amplitude of oscillation
$a$	=	cylinder diameter
$C_p$	=	pressure coefficient
$C_x$	=	force coefficient in the $x$ direction
$C_y$	=	force coefficient in the $y$ direction
$c$	=	chord
$dt$	=	time step
$F_x$	=	$X$ component of the resultant pressure force acting on the vehicle
$F_y$	=	$Y$ component of the resultant pressure force acting on the vehicle
$f, g$	=	generic functions
$h$	=	height
$i$	=	time index during navigation
$j$	=	waypoint index
$K$	=	trailing-edge (TE) nondimensional angular deflection rate

## I. Introduction

Jet Propulsion Laboratory is developing a two-phase mechanically pumped fluid loop (2PMPFL) thermal control system to enable novel mission designs and greater science return for NASA. Pumped two-phase fluid loops have the potential to provide robust and effective thermal control that combine the best aspects of passive two-phase systems (heat pipes) and mechanically pumped single-phase fluid loops. The current requirements include the development of a system with multiple 1 m<sup>2</sup> evaporators, each of which is capable of remaining spatially and temporally isothermal

---

<sup>1</sup> Thermal Engineer, Propulsion, Thermal, and Materials Engineering Section, 4800 Oak Grove Dr., Pasadena, CA 91109.

<sup>2</sup> Technologist, Propulsion, Thermal, and Materials Engineering Section, 4800 Oak Grove Dr., Pasadena, CA 91109

<sup>3</sup> Mechanical Engineer, Propulsion, Thermal, and Materials Engineering Section, 4800 Oak Grove Dr., Pasadena, CA 91109

<sup>4</sup> Principal Engineer, Propulsion, Thermal, and Materials Engineering Section, 4800 Oak Grove Dr., Pasadena, CA 91109

<sup>5</sup> Thermal Engineer, Propulsion, Thermal, and Materials Engineering Section, 4800 Oak Grove Dr., Pasadena, CA 91109.

while accommodating heat loads of up to 500 W and local fluxes of up to 5 W/cm<sup>2</sup>. The goal is to attain this using less than 5 W of power. Such a system would be able to accommodate the next generation of payload and bus electronics while using minimal resources.

In its simplest form, the 2PMPFL consists of an evaporator, condenser, accumulator, and pump. During normal operation, the pump supplies liquid to the evaporator where the heat load is applied. In the evaporator, the working fluid starts boiling and becomes vapor-liquid two-phase flow. This vapor-liquid two-phase then flows to the condenser where heat is removed and the fluid is re-condensed. The accumulator regulates the system pressure. The temperature of the evaporator becomes close to saturation temperature of the accumulator. This simplest form of 2PMPFL is called Mixed Flow Architecture (MFA).

Another form of the 2PMPFL is Separated Flow Architecture (SFA). The SFA is a pump-assisted Capillary Pumped Loop (CPL) with liquid bypass line. In this system, the evaporator has porous material called wick which separates the vapor phase and the liquid phase. Only vapor leaves the evaporator during normal operation. The pump moves liquid phase to the evaporator and to the liquid bypass line. In the evaporator, the working fluid is vaporized. The bypass line provides an alternate flow path and ensures that excess liquid is not pushed into the evaporator by the pump. This allows the fluid flow in the evaporator to be regulated by the wick, which only draws in the liquid that it needs to accommodate the heat load via capillary pumping. This SFA has several merits compared with MFA. SFA systems are more predictable and amenable to analysis than MFA systems, since the region of two-phase flow, which is difficult to predict in micro-gravity, can be minimized in the system. Additionally, for a given level of performance (power level, isothermality) an SFA system requires less power than an MFA system since no pre-heater is required for nominal operation. Finally, producing an isothermal evaporator is more feasible with an SFA system because the wick-type evaporator has possibility to achieve highest heat transfer coefficient.

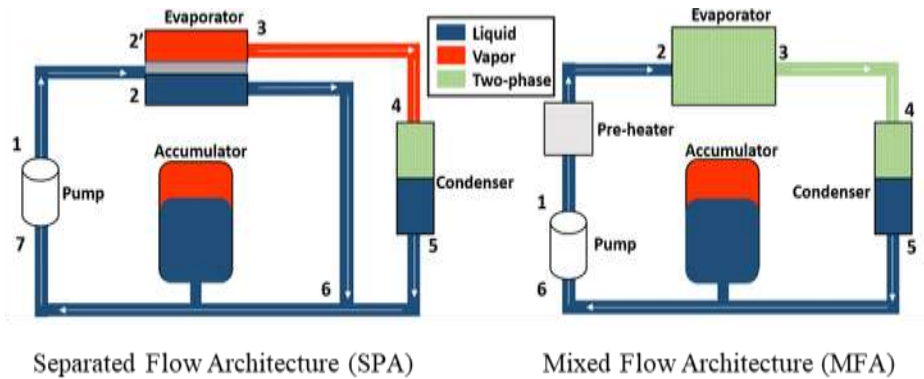


Figure 1. Types of Two-Phase Mechanically Pumped Fluid Loop (2PMPFL).

## II. Evaporator Design Concept

At the heart of the 2PMPFL is the evaporator. In previous studies, we have developed several types of evaporators. The first evaporator was fabricated using traditional manufacturing techniques (Figure 2). The heating plate has pillars and wick is held on top of those pillars. This first proto-type evaporator could accommodate 390 W while maintaining the evaporator surface within a band of 3°C, but it had some critical limitations in its design including an inability to hold substantial pressure and an O-ring seal based assembly that is only suitable for ground testing. In addition, the tortuous path for heat conduction through the pillars to vapor-liquid interface was not optimized design.

For the second and third proto-types of the evaporator, additive manufacturing was used for fabrication method. The JPL developed method to print porous material by Direct Metal Laser Sintering (DMLS). By utilizing additive manufacturing, the evaporator can be fabricated as monolithic piece. This solves many of the issues seen in the previous evaporator. The purpose of second evaporator proto-type was to test that the various aspects of a DMLS evaporator would in fact all work as expected (e.g. the wick and the casing structure), and that the key elements could indeed be fabricated as designed. Evaporator #1 was designed for use in a low pressure (below atmospheric pressure), 2PMPFL system using FC-72 as the working fluid.

The third prototype was developed to demonstrate a more optimal design that would be closer to the anticipated flight-like evaporator (Figure 3). It was designed for use in an ammonia 2PMPFL with maximum operating pressures of 1.39 MPa, and had a thinner form factor. To accommodate the high pressure, structural pillars were included that

spanned the planar faces of the evaporator. The thinner form factor was achieved by making smaller port holes and powder drain holes that could be connected to or plugged via welding. The wicking structure had the same properties as that used in the second evaporator.

In term of thermal design, the wick is contacted on entire heating plate and vapor-liquid interface (meniscus) is formed within the wick under the heating plate. However, this causes two problems. The first problem is that the vapor pocket is formed under the heating plate and the heat transfer path to the vapor-liquid interface, which is controlled at the saturation temperature, becomes tortuous. The second problem was pressure loss in vapor flow, which is generated at the meniscus, because this has to flow the wick firstly to reach the vapor channels.

Recently, Odagiri proposed high thermal performance evaporator for Loop Heat Pipes. In his studies, it was found that the heat transfer coefficient from the heating plate where the heat load is actually applied to the vapor is enhanced by existence of the liquid bridge, which forms in vapor grooves as shown in Figure 4. This liquid bridge produce the pressure increase and changes its radius as required pressure increase changes. The heat is transferred from the heating plate to vapor-liquid interface through the very thin liquid film. Thus heat transfer coefficient becomes incredibly high. In addition, it was reported the heat transfer coefficient is even improved in moderate heat flux mode where nucleate boiling occurs at the interface between the heating plate and the wick fins. However, this heat transfer coefficient decreases drastically in high heat flux mode where the liquid bridges disappear and vapor pocket is formed at heating plate-wick fin interface. Therefore, the concept of new evaporator design is to utilize the high heat transfer coefficient in low and moderate heat flux modes.

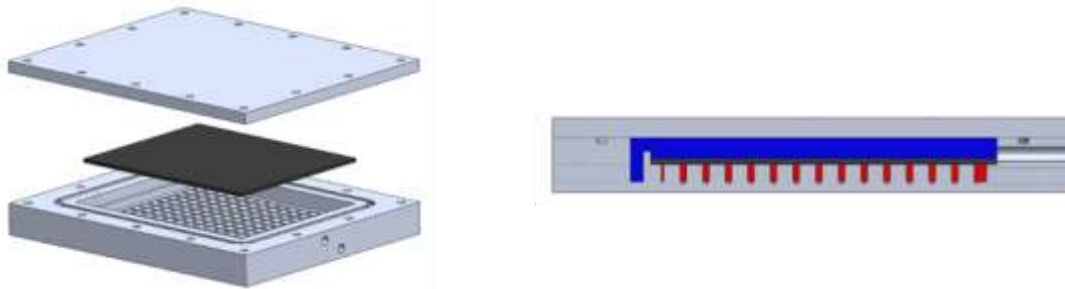


**Figure 2. First Proto-type of Evaporator Fabricated Using Traditional Manufacturing Techniques.** *The vapor channel (red), is separated from the liquid channel (blue) by the wick (black).*

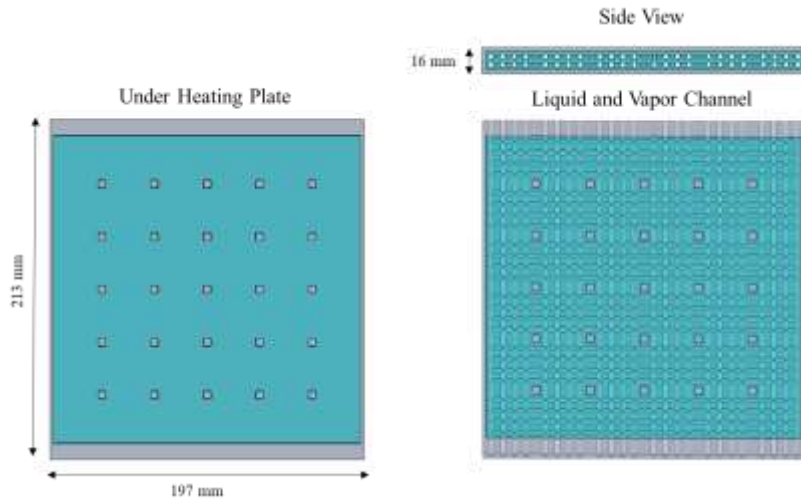


**Figure 3. Third Proto-type of Evaporator Fabricated Using Additive Manufacturing.** *The wick (light blue) and solid part (gray) are fabricated in single piece.*

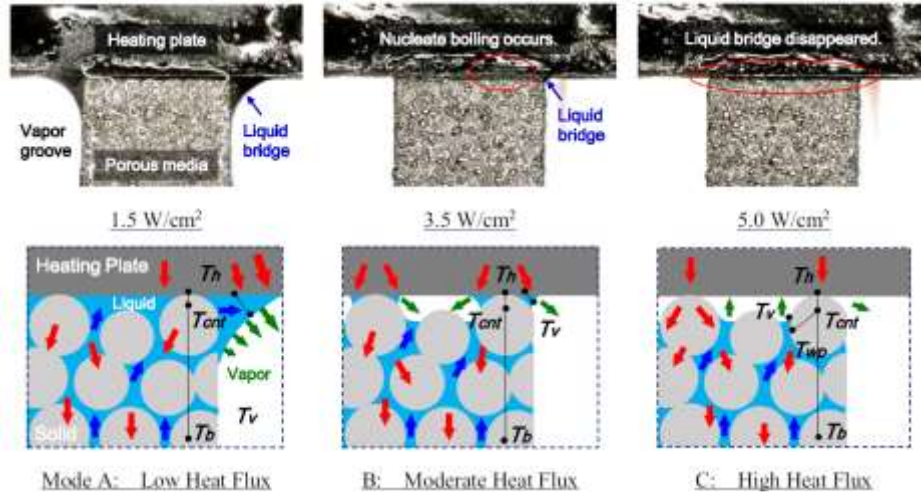


Figure 4. Microscopy images and three types of liquid–vapor interface behavior presented by Odagiri.<sup>00</sup>

### III. Operational Range Calculation

#### A. Capillary Limit

The operational limit of the SFA is capillary limit. If the required pressure increase in the evaporator exceeds the maximum pressure which the meniscus can hold in the wick, the vapor phase penetrates from the vapor channel to the liquid channel and this causes unstable operation of the system. Moreover, this eventually ends up the superheat in the evaporator and dry out. The maximum pressure, which the meniscus can hold, is described in Eq1. In this equation, the pore radius is important as property of wick material.

$$2\sigma/r \cos(\theta).$$

JPL has capability to print the porous material by 3D printer. Material is aluminum, titanium, stainless steel, and Inconel. For this evaporator, we chose aluminum for the material, because aluminum has the advantage in term of lightweight, high thermal conductivity. Figure 5(a) shows the wick properties which can be fabricated in JPL. The pore radius can vary from 3  $\mu\text{m}$  to 28  $\mu\text{m}$ . Also, it is obvious that the permeability decreases with decreases of pore radius size. For the evaporator, permeability is also important parameter in addition to the pore radius because pressure loss within the wick increases with permeability. Ideally, the smallest pore radius is desirable in term of the operational limit. However, permeability of sample which has smallest pore radius is very low as  $1 \times 10^{-14}$ . Therefore, we chose the sample marked by red circle which has larger pore radius but higher permeability. Figure 5(b) shows the SEM image of the sample, which has similar property of chosen porous material. The majority of the structure is 100  $\mu\text{m}$  scale, but also there are balls and holes smaller than 100 $\mu\text{m}$ . The effective pore radius of chosen porous material is 18  $\mu\text{m}$ , permeability is  $3.2 \times 10^{-13}$ , and porosity is 22.3%.

The required pressure increase in the evaporator is affected by the heat load applied into the evaporator, length of the vapor line, and the configuration of the evaporator. Because mass flow rate into the evaporator increases almost lineally with the heat load to remove the heat by latent heat, pressure loss in the vapor line increases with the heat load. To predict the required pressure increase, the system level transient model has been developed. The model is based on the one-dimensional compressive Navier-Stokes equations (ref). The code is written in Fortran and it is linked with the REFPROP thermal fluid property database. The model can predict temperature, pressure, and velocity of the fluid at any locations in the loop. In addition, mass flowrate into the evaporator and liquid bypass line are calculated based on the flow resistance in each line. Picture of the simulated test bed was shown in Figure 6. In this simulation, the evaporator, condenser, and sub cooler are modeled in one node respectively. The pressure loss in the evaporator is omitted because the configuration is not decided yet.

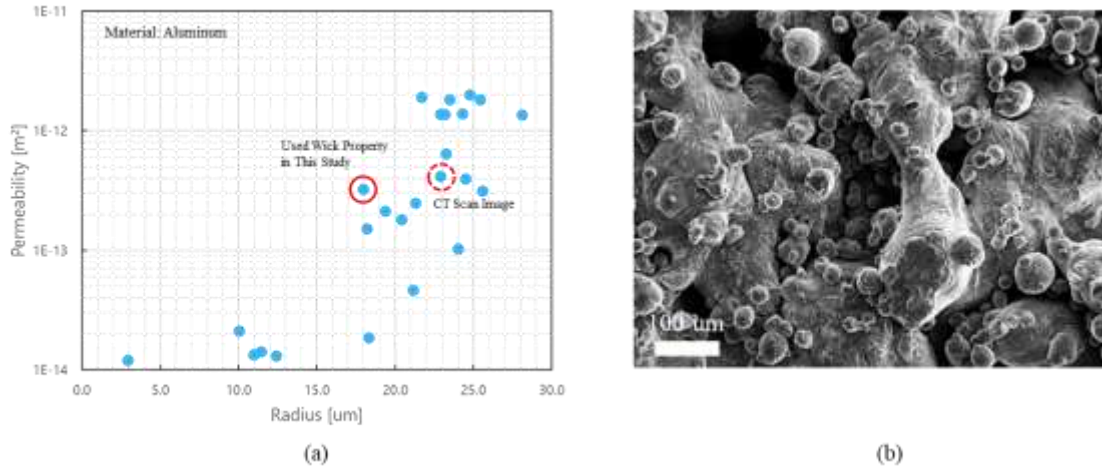


**Figure 5. (a) Wick Properties Available in Direct Metal Laser Sintering. (b) SEM Image of the Sample.**

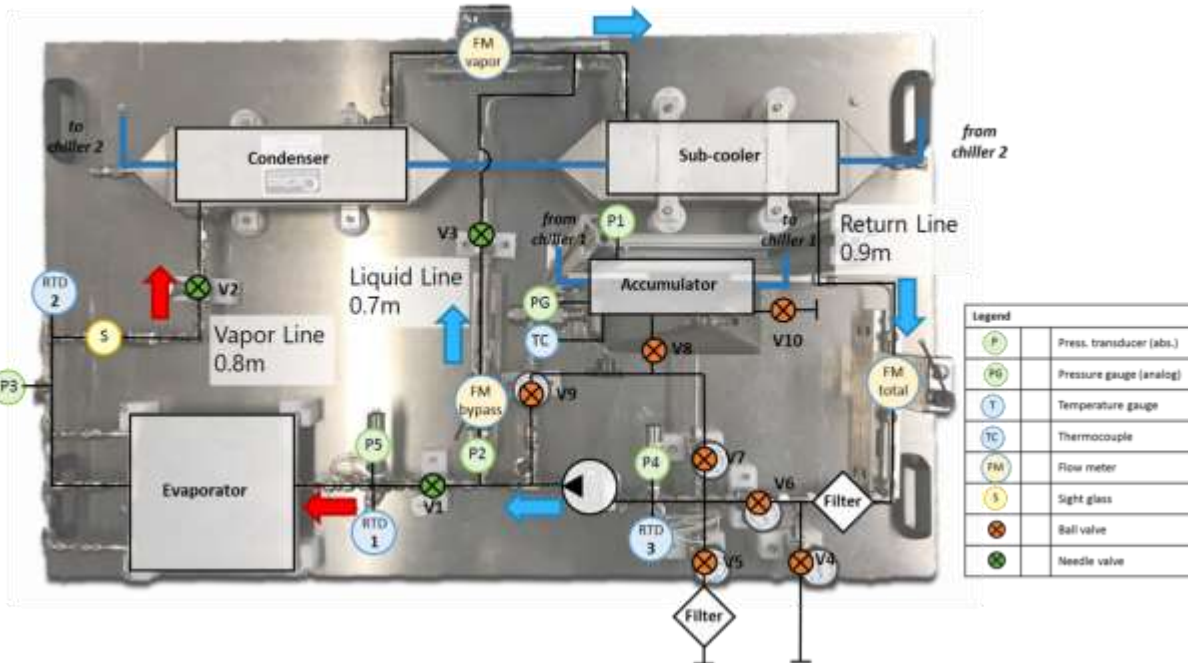


**Figure 6. Schematic of Two-Phase Mechanically Pumped Loop (2PMPFL) Testbed.**

Figure 7 shows the pressure profile in the loop in the case of the 500W with 0.003 kg/s. The entire pressure decreases along the loop and recover in the pump, but the highest pressure in the loop is in the evaporator. This pressure increase is consumed along the vapor line and it is balanced at the vapor liquid junction after the condenser. This pressure increase is created at the vapor liquid interface. Once this this pressure increase exceeds the maximum pressure held by wick, the vapor phase penetrate into the liquid side, and this is the operational limit of the loop.

Figure 8 shows the required pressure increase in the evaporator versus the heat inputs in different mass flow rate. The minimum heat input limit is the required heat input to create the separated flow mode. In the result, the operational range of mass flow rate 0.003kg/s is widest as from 400W to 1100W. In the smaller mass flow rate 0.001, the minimum mass flowrate is lower and it reaches to the maximum heat input at 600W. This maximum heat input is dry-out, which means the total mass flow rate is not enough to accommodate the heat input. In the higher mass flow rate, the minimum heat input is higher and maximum heat input is higher too, but the operational heat input range is narrower than the case of 0.003kg/s. Therefore we chose 0.003 kg/s case as baseline.



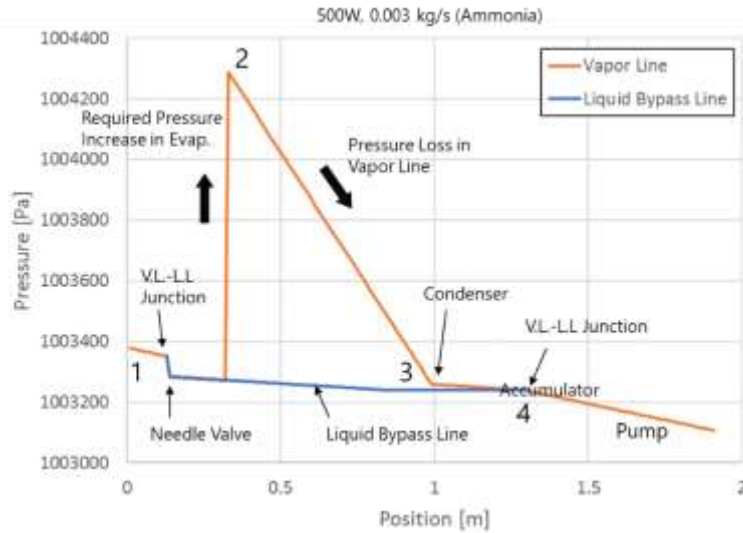


Figure 7. Pressure Profile in the Loop (500W, 0.003 kg/s).

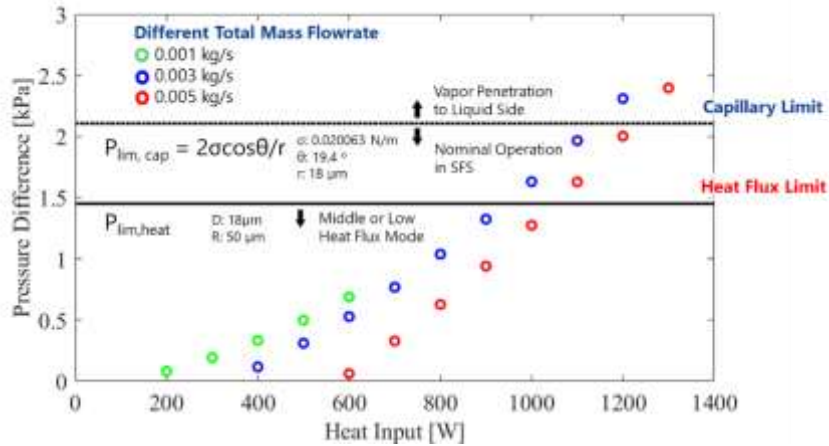


Figure 8. Required Pressure Increase in Evaporator.

### B. Heat Flux Limit

There is another operational limit. The heat transfer coefficient decreases drastically from the moderate heat flux mode to the high heat flux mode. Therefore, the operational range is desired to be within the moderate heat flux mode. The transition from the moderate to high heat input mode was modeled by Oka (Ref). In this transition, the disappearance of the liquid bridge between the heating plate and the wick pillars is the critical. The liquid bridge shown in Figure 9 disappears at pressure difference described in Eq XX. The bulk structure size and the gap size are important for this pressure. Our evaporator is fabricated as monolithic piece by additive manufacturing and there are no significant gap between the heating plate and the wick. Thus, for the calculation, the pore radius 18  $\mu\text{m}$  was used as the size of gap and 50  $\mu\text{m}$  was used for the radius of the structure. These values results in the transition pressure is around 1.5 kPa. This results in the operational range in low or moderate heat flux mode from 400W to 900W in Figure 8.

$$P_{\text{cap}} = \sigma \left( \frac{1}{r_1} + \frac{1}{r_2} \right) \quad (2)$$

$$r_1 = \frac{D + d}{\cos\theta_1 + \cos(\theta_2 + \alpha)} \quad (3)$$

$$r_2 = R\sin\alpha + r_1 \{ \sin(\theta_2 + \alpha) - 1 \} \quad (4)$$

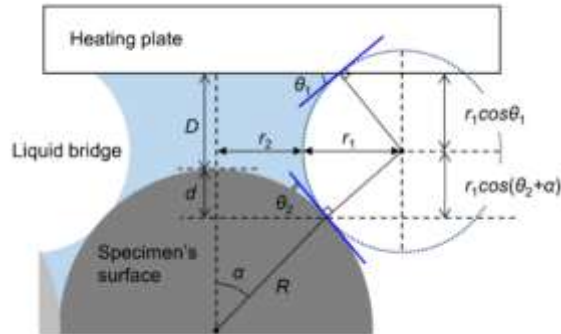
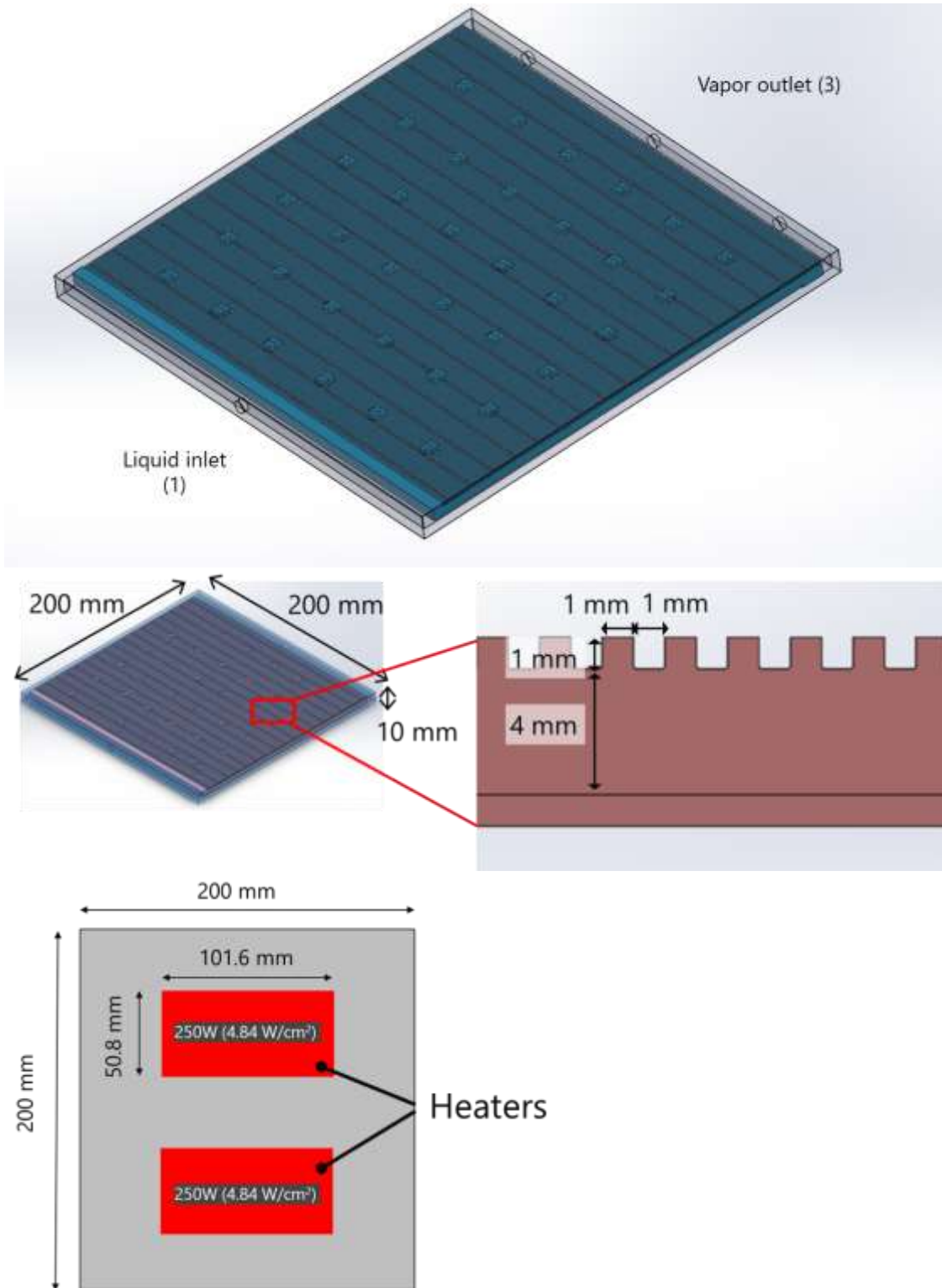


Figure 9. Schematic of Liquid Bridge between Heating Plate and Wick.<sup>00</sup>

#### IV. Evaporator Performance Calculation

In the previous study by Odagiri, it was found that the thermal performance of the evaporator is improved as the triple phase contact line (TPCL) between liquid, vapor, and heating plate becomes longer (RefXX). Thus, the fin width and groove width are designed as narrow as possible. Constrain is the resolution of the DMLS. In the current technology, 1mm is reasonable for the minimum feature resolution. Therefore, the height and width of the fin, and width of the groove were designed as 1 mm. The height of the wick base is 4mm and height of the liquid reservoir is 1mm respectively. Figure XX shows the entire evaporator design and wick geometry. In addition to the solid casing and wick, the evaporator has the solid pillars between the top heating plate and the bottom plate to increase the structural strength. This pillar design was optimized through design itarration using structural analysis and the evaporator can hold pressure up to XX MPa in nominal operation. Figure XX shows the heater arrangement. Because the heat flux is changed by the size of the heaters, the arrangement is designed in advance.



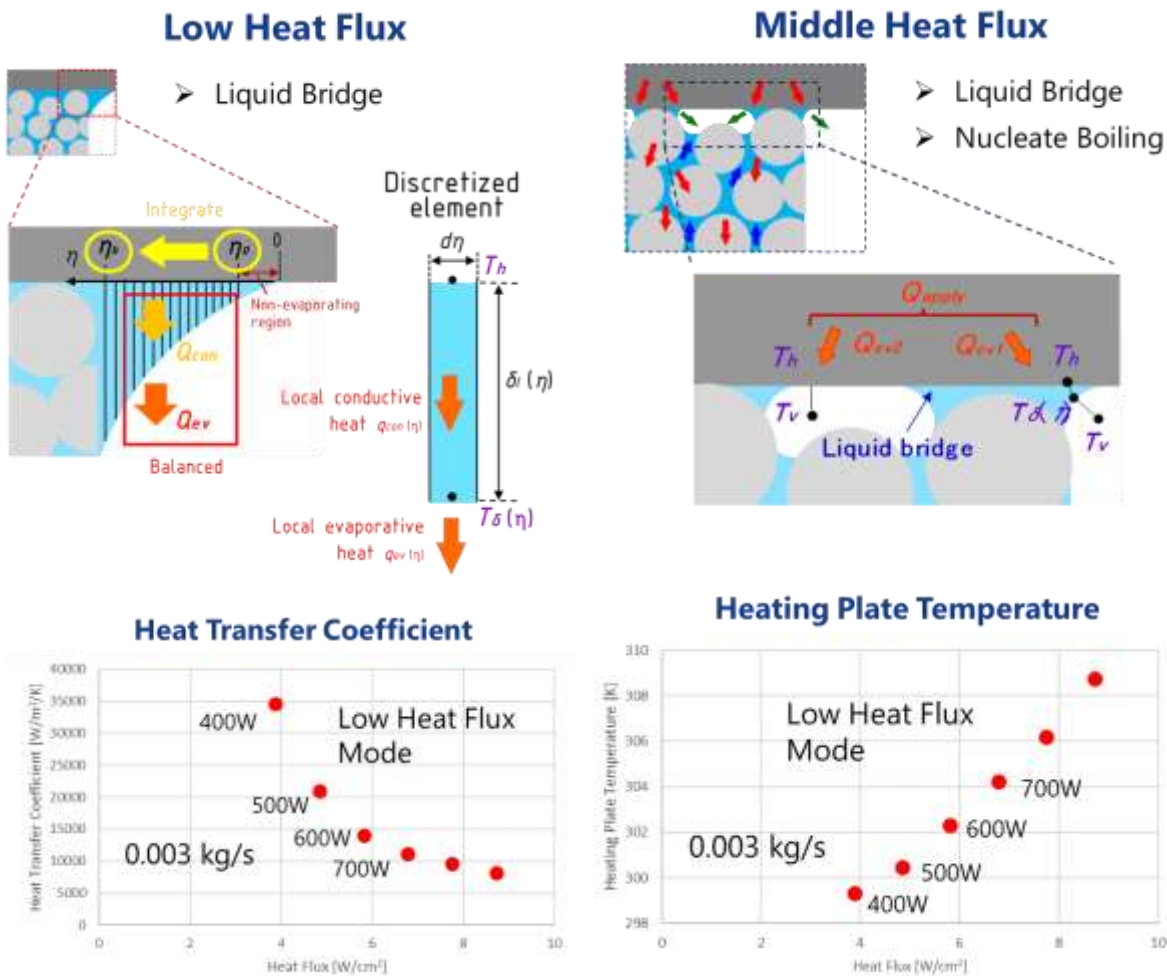
The heat transfer can be calculated the model proposed by Odagiri (2017). The detail of the model is described in Reference XX. The model is different in the each mode of low, moderate, and high heat flux. In low heat flux mode,



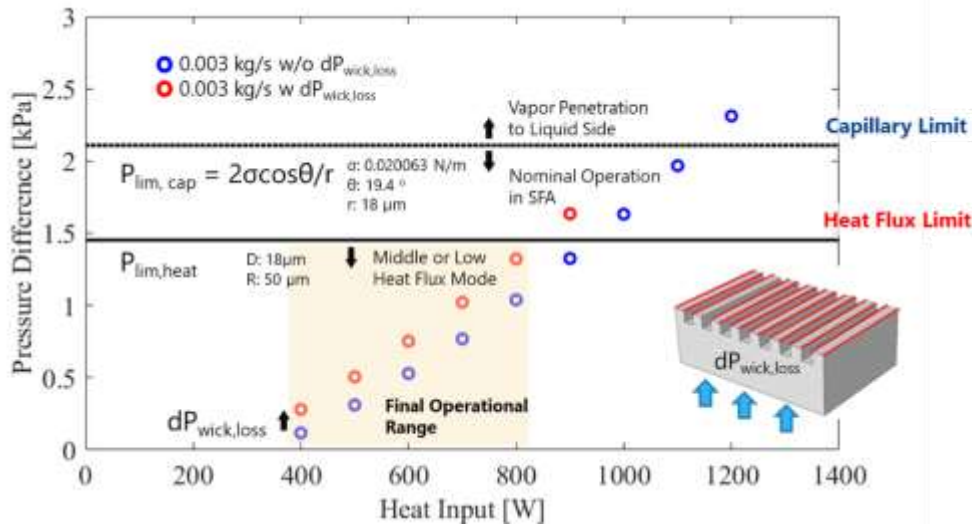
the conduction through the liquid bridge is calculated. The radius of the liquid bridge is calculated based on only the pressure loss within the wick in previous study, but in this study liquid bridge radius is determined from both of the pressure loss with in the wick and required pressure increase in the evaporator because the actual evaporator performance in the loop can be calculated in this way. In addition, the entire shape of the liquid bridge is determined by the contact angle between liquid and heating plate, and wick material.

In the moderate heat input mode, the nucleate boiling occurs at the interface between the heating plate and the wick in addition to the heat conduction through the liquid film. The amount of the heat goes to liquid film and goes to the boiling are balanced depending on the heat transfer coefficient of these two factors. In the transition between the low heat flux and moderate heat flux mode is determined by the contributions of each factor.

The estimated heat transfer coefficient is shown in the figure. The heat transfer coefficient ranges from 8000 to 35000 W/m<sup>2</sup>/K. The heat transfer coefficient decreases with the increase of the input heat flux because the smaller liquid bridge radius is required to crease higher pressure increase at higher heat input, and effective length of the liquid film becomes shorter.



To calculate the final operation range, the pressure loss in the wick is added to the required pressure increase in the evaporator. This results in the final operation range from 400W to 800W which corresponds to 4 W/cm<sup>2</sup> to 7.8 W/cm<sup>2</sup> with given heater sizes.



## V. Conclusion

A conclusion section is not required, though it is preferred. Although a conclusion may review the main points of the paper, do not replicate the abstract as the conclusion. A conclusion might elaborate on the importance of the work or suggest applications and extensions. *Note that the conclusion section is the last section of the paper that should be numbered. The appendix (if present), acknowledgment, and references should be listed without numbers.*

## Acknowledgments

The research was carried out at the Jet Propulsion Laboratory, California Institute of Technology, under a contract with the National Aeronautics and Space Administration.

## References

<sup>1</sup>Vatistas, G. H., Lin, S., and Kwok, C. K., "Reverse Flow Radius in Vortex Chambers," *AIAA Journal*, Vol. 24, No. 11, 1986, pp. 1872, 1873.

<sup>2</sup>Dornheim, M. A., "Planetary Flight Surge Faces Budget Realities," *Aviation Week and Space Technology*, Vol. 145, No. 24, 9 Dec. 1996, pp. 44-46.

<sup>3</sup>Terster, W., "NASA Considers Switch to Delta 2," *Space News*, Vol. 8, No. 2, 13-19 Jan. 1997, pp., 1, 18.

All of the preceding information is required. The journal issue number ("No. 11" in Ref. 1) is preferred, but the month (Nov.) can be substituted if the issue number is not available. Use the complete date for daily and weekly publications. Transactions follow the same style as other journals; if punctuation is necessary, use a colon to separate the transactions title from the journal title.

### Books

<sup>4</sup>Peyret, R., and Taylor, T. D., *Computational Methods in Fluid Flow*, 2<sup>nd</sup> ed., Springer-Verlag, New York, 1983, Chaps. 7, 14.

<sup>5</sup>Oates, G. C. (ed.), *Aerothermodynamics of Gas Turbine and Rocket Propulsion*, AIAA Education Series, AIAA, New York, 1984, pp. 19, 136.

<sup>6</sup>Volpe, R., "Techniques for Collision Prevention, Impact Stability, and Force Control by Space Manipulators," *Teleoperation and Robotics in Space*, edited by S. B. Skaar and C. F. Ruoff, Progress in Astronautics and Aeronautics, AIAA, Washington, DC, 1994, pp. 175-212.

Publisher, place, and date of publication are required for all books. No state or country is required for major cities: New York, London, Moscow, etc. A differentiation must always be made between Cambridge, MA, and Cambridge, England, UK. Note that series titles are in roman type.